SECOND-ORDER PERFORMANCE ANALYSIS OF STANDARD ESPRIT

Jens Steinwandt [1], *Florian Roemer* [2,3], *and Martin Haardt* [1]

[1] Communications Research Laboratory, Ilmenau University of Technology, P.O. Box 100565, 98684 Ilmenau, Germany
[2] Digital Broadcasting Research Laboratory, Ilmenau University of Technology, P.O. Box 100565, 98684 Ilmenau, Germany
[3] Fraunhofer Institute for Integrated Circuits IIS
{jens.steinwandt, florian.roemer, martin.haardt}@tu-ilmenau.de, www.tu-ilmenau.de/crl

ABSTRACT

This paper provides a second-order (SO) analytical performance analysis of the 1-D Standard ESPRIT algorithm. Existing performance analysis frameworks are based on first-order (FO) approximations of the parameter estimation error, which are asymptotic in the effective signal-to-noise ratio (SNR), i.e., they become exact for either high SNRs or a large sample size. However, these FO expressions do not capture the algorithmic behavior in the threshold region at low SNRs or for a small sample size. Yet, such conditions are often encountered in practice. Therefore, we present a closed-form expression for the parameter estimation error of 1-D Standard ESPRIT up to the SO that is valid in a wider effective SNR range. Moreover, we derive an analytical mean square error (MSE) expression, where we assume a zero-mean circularly symmetric complex Gaussian noise distribution. Finally, we use the existing FO MSE expression and the derived SO MSE expression to analytically compute the SNR breakdown threshold of the MSE threshold region. Empirical simulations verify the analytical expressions.

Index Terms— ESPRIT, performance analysis, second-order, DOA estimation.

1. INTRODUCTION

Direction of arrival (DOA) estimation of impinging signals is a task required in many array processing applications including radar, sonar, mobile communications, etc. Due to their simplicity and high-resolution capabilities, ESPRIT-type algorithms [1, 2] are among the most popular subspace-based parameter estimation schemes.

The analytical performance of ESPRIT-type algorithms, which is of interest for performance prediction and objective comparison purposes, has been thoroughly studied in the literature [3, 4, 5, 6]. The two most established frameworks for the perturbation due to measurement noise have been reported in [3] and [4]. Both concepts rely on first-order (FO) approximations of the perturbed data. While [3] employs a statistical approach based on the eigenvector distribution that is only asymptotic in the sample size, [4] presents a deterministic approach by analytically modeling the subspace perturbation. The latter is more general as it is asymptotic in the effective signal-to-noise ratio (SNR), i.e, the analytical expressions become exact for either high SNRs or a large sample size. Multi-dimensional extensions of [4] and the incorporation of additional signal structure, i.e., strict non-circularity, have been considered in [5] and [6], respectively.

This work was partially supported by the DFG project EXPRESS (HA 2239/6-1) and the Carl-Zeiss Foundation under the scholarship project EMBiCoS.

The drawback of the existing FO perturbation frameworks is that the perturbation model of the noise is only a FO approximation. As a result, the analytical expressions are only valid in the high effective SNR region and therefore, do not capture the behavior of the algorithms in the threshold region at low SNRs or for a small sample size. Yet, these are the conditions that are most often encountered in practice. This aspect motivates the development of performance analysis frameworks that also take into account the second-order (SO) perturbation of the noise such that the analytical results are valid in a wider effective SNR range. An extension of the FO results on the subspace estimation error in [4] to the SO case has been derived in [7, 8]. The analytical SO performance of MUSIC in the presence of array modeling errors has been provided in [9] and an SO bias analysis of Standard ESPRIT has been presented in [7]. To the best of our knowledge, the SO performance analysis with respect to the mean square error (MSE) of ESPRIT-type algorithms is still open.

Another important performance-related research aspect is the characterization of the threshold region. The threshold region refers to a rapid deterioration of the MSE of parameter estimators, i.e., a performance breakdown, when the SNR falls below a threshold SNR. The threshold region and its breakdown SNR has been investigated for the maximum likelihood (ML) estimator in [10, 11]. However, the threshold SNR of ESPRIT-type algorithms has so far not been studied in the literature.

In this paper, we present a SO performance analysis of 1-D Standard ESPRIT using the simple least squares (LS) solution of the shift-invariance equations. We derive a closed-form SO approximation for the estimation error in terms of the explicit noise realization based on the results in [7, 8]. Moreover, we find an analytical MSE expression under the simplifying assumption of a zero-mean circularly symmetric complex Gaussian noise distribution. It is apparent that the derived expressions agree with those in [5], if only the FO terms are maintained. Finally, we use the existing FO MSE expression from [5] and the derived SO MSE expression in this work to analytically compute the threshold SNR for the threshold region. Numerical simulation results verify the derived analytical expressions.

2. DATA MODEL

Let d planar wavefronts from narrowband far-field sources impinge on a shift-invariant array composed of M identical sensor elements. The collection of N data snapshots can be modeled by the measurement matrix

$$\boldsymbol{X} = \boldsymbol{A}\boldsymbol{S} + \boldsymbol{N} = \boldsymbol{X}_0 + \boldsymbol{N} \in \mathbb{C}^{M\times N}, \tag{1}$$

where the array steering matrix $\boldsymbol{A} = [\boldsymbol{a}(\mu_1), \ldots, \boldsymbol{a}(\mu_d)] \in \mathbb{C}^{M\times d}$ contains the array steering vectors $\boldsymbol{a}(\mu_i)$ that correspond to the i-th spatial frequency $\mu_i,\ i = 1, \ldots, d$. Moreover, $\boldsymbol{S} \in \mathbb{C}^{d \times N}$ is the symbol matrix and $\boldsymbol{N} \in \mathbb{C}^{M \times N}$ represents the additive zero-mean circularly symmetric white Gaussian sensor noise with variance σ_{n}^2.

Due to the shift invariance structure of the array, we can apply ESPRIT-type algorithms to estimate the desired spatial frequencies. Specifically, we have $\boldsymbol{J}_1 \boldsymbol{A} \boldsymbol{\Phi} = \boldsymbol{J}_2 \boldsymbol{A}$, where $\boldsymbol{J}_1, \boldsymbol{J}_2 \in \mathbb{R}^{M^{(\mathrm{sel})} \times M}$ are the selection matrices that select $M^{(\mathrm{sel})}$ out of M sensors for each of the two subarrays and $\boldsymbol{\Phi} = \mathrm{diag}\{\mathrm{e}^{\mathrm{j}\mu_i}\}_{i=1}^d \in \mathbb{C}^{d \times d}$ contains the spatial frequencies of interest.

Since $\boldsymbol{A}$ is unknown, the signal subspace $\hat{\boldsymbol{U}}_{\mathrm{s}} \in \mathbb{C}^{M \times d}$ is estimated by computing the d dominant left singular vectors of $\boldsymbol{X}$. Then, a non-singular matrix $\boldsymbol{T} \in \mathbb{C}^{d \times d}$ can be found such that $\boldsymbol{A} \approx \hat{\boldsymbol{U}}_{\mathrm{s}} \boldsymbol{T}$. Using this relation, the shift invariance equation can be expressed in terms of the estimated signal subspace, yielding

$$\boldsymbol{J}_1 \hat{\boldsymbol{U}}_{\mathrm{s}} \boldsymbol{\Psi} \approx \boldsymbol{J}_2 \hat{\boldsymbol{U}}_{\mathrm{s}} \tag{2}$$

with $\boldsymbol{\Psi} \approx \boldsymbol{T} \boldsymbol{\Phi} \boldsymbol{T}^{-1}$. Often, the unknown matrix $\boldsymbol{\Psi}$ is estimated using least squares (LS), i.e., $\hat{\boldsymbol{\Psi}} = (\boldsymbol{J}_1 \hat{\boldsymbol{U}}_{\mathrm{s}})^+ \boldsymbol{J}_2 \hat{\boldsymbol{U}}_{\mathrm{s}} \in \mathbb{C}^{d \times d}$, where $(\cdot)^+$ stands for the Moore-Penrose pseudo inverse. Finally, the spatial frequency estimates are obtained by $\hat{\mu}_i = \arg\{\hat{\lambda}_i\},\ i = 1, \ldots, d$, where $\hat{\lambda}_i$ are the eigenvalues of $\hat{\boldsymbol{\Psi}}$.

3. SECOND-ORDER PERFORMANCE ANALYSIS OF STANDARD ESPRIT

The presented SO performance analysis is based on the assumption that the noise-free signal is superimposed by a small additive noise contribution. Then, the derivation of the SO expansion of Standard ESPRIT follows similar steps as for the FO expansion from [4, 5] but additionally takes into account the SO terms that are neglected by the FO analysis. The steps for Standard ESPRIT include the SO perturbation of the signal subspace $\Delta \boldsymbol{U}_{\mathrm{s}}$ in terms of the noise $\boldsymbol{N}$, which was already derived in [8], the SO perturbation of the LS solution $\Delta \boldsymbol{\Psi}$ with respect to $\Delta \boldsymbol{U}_{\mathrm{s}}$, the SO eigenvalue perturbation $\Delta \lambda_i$ in terms of $\Delta \boldsymbol{\Psi}$, and the SO perturbation of the spatial frequencies $\Delta \mu_i$ as a function of $\Delta \lambda_i$. Note that similar expressions have also been found for the bias analysis in [7]. Here, however, we derive the analytical MSE expression and the threshold SNR.

3.1. Perturbation of the Signal Subspace

We first consider the signal subspace estimation error due to the small additive perturbation $\boldsymbol{N}$. To this end, we extract the noise-free subspaces from $\boldsymbol{X}_0$ as

$$\boldsymbol{X}_0 = \begin{bmatrix} \boldsymbol{U}_{\mathrm{s}} & \boldsymbol{U}_{\mathrm{n}} \end{bmatrix} \begin{bmatrix} \boldsymbol{\Sigma}_{\mathrm{s}} & \boldsymbol{0} \\ \boldsymbol{0} & \boldsymbol{0} \end{bmatrix} \begin{bmatrix} \boldsymbol{V}_{\mathrm{s}} & \boldsymbol{V}_{\mathrm{n}} \end{bmatrix}^{\mathrm{H}}, \tag{3}$$

where $\boldsymbol{U}_{\mathrm{s}} \in \mathbb{C}^{M \times d}$, $\boldsymbol{U}_{\mathrm{n}} \in \mathbb{C}^{M \times (M-d)}$, as well as $\boldsymbol{V}_{\mathrm{s}} \in \mathbb{C}^{N \times d}$ span the signal subspace, the noise subspace, and the row space respectively, and $\boldsymbol{\Sigma}_{\mathrm{s}} \in \mathbb{R}^{d \times d}$ contains the non-zero singular values on its diagonal. Modeling the estimated signal subspace as $\hat{\boldsymbol{U}}_{\mathrm{s}} = \boldsymbol{U}_{\mathrm{s}} + \Delta \boldsymbol{U}_{\mathrm{s}}$, where $\Delta \boldsymbol{U}_{\mathrm{s}}$ denotes the subspace estimation error, we obtain the SO approximation [7, 8]

$$\Delta \boldsymbol{U}_{\mathrm{s}} = \Delta \boldsymbol{U}_{\mathrm{s}}^{(1)} + \Delta \boldsymbol{U}_{\mathrm{s}}^{(2)} + \mathcal{O}\{\delta^3\}, \tag{4}$$

where $\Delta \boldsymbol{U}_{\mathrm{s}}^{(1)}$ is the FO perturbation in terms of $\boldsymbol{N}$, given as [4]

$$\Delta \boldsymbol{U}_{\mathrm{s}}^{(1)} = \boldsymbol{U}_{\mathrm{n}} \boldsymbol{U}_{\mathrm{n}}^{\mathrm{H}} \boldsymbol{N} \boldsymbol{V}_{\mathrm{s}} \boldsymbol{\Sigma}_{\mathrm{s}}^{-1}, \tag{5}$$

and $\Delta \boldsymbol{U}_{\mathrm{s}}^{(2)}$ denotes the SO perturbation in terms of $\boldsymbol{N}$, given by [8]

$$\begin{aligned} \Delta \boldsymbol{U}_{\mathrm{s}}^{(2)} = &-\boldsymbol{U}_{\mathrm{n}} \boldsymbol{U}_{\mathrm{n}}^{\mathrm{H}} \boldsymbol{N} \boldsymbol{X}_0^+ \boldsymbol{N} \boldsymbol{V}_{\mathrm{s}} \boldsymbol{\Sigma}_{\mathrm{s}}^{-1} \\ &+ \boldsymbol{U}_{\mathrm{n}} \boldsymbol{U}_{\mathrm{n}}^{\mathrm{H}} \boldsymbol{N} \boldsymbol{V}_{\mathrm{n}} \boldsymbol{V}_{\mathrm{n}}^{\mathrm{H}} \boldsymbol{N}^{\mathrm{H}} \boldsymbol{U}_{\mathrm{s}} \boldsymbol{\Sigma}_{\mathrm{s}}^{-2}. \end{aligned} \tag{6}$$

Further, we have $\delta = \|\boldsymbol{N}\|$, and $\|\cdot\|$ represents a submultiplicative norm. In what follows, we define $(\cdot)^{(1)}$ and $(\cdot)^{(2)}$ as the FO and SO approximations, respectively.

3.2. Perturbation of the Shift Invariance Solution

For the shift invariance solution, we write $\hat{\boldsymbol{\Psi}} = \boldsymbol{\Psi} + \Delta \boldsymbol{\Psi}$ such that the shift invariance equation in (2) can be written as $\boldsymbol{J}_1 (\boldsymbol{U}_{\mathrm{s}} + \Delta \boldsymbol{U}_{\mathrm{s}}) (\boldsymbol{\Psi} + \Delta \boldsymbol{\Psi}) \approx \boldsymbol{J}_2 (\boldsymbol{U}_{\mathrm{s}} + \Delta \boldsymbol{U}_{\mathrm{s}})$. Then, the perturbation of the LS solution up to the SO is given by

$$\Delta \boldsymbol{\Psi} \approx \big(\boldsymbol{J}_1 (\boldsymbol{U}_{\mathrm{s}} + \Delta \boldsymbol{U}_{\mathrm{s}})\big)^+ (\boldsymbol{J}_2 \Delta \boldsymbol{U}_{\mathrm{s}} - \boldsymbol{J}_1 \Delta \boldsymbol{U}_{\mathrm{s}} \boldsymbol{\Psi}). \tag{7}$$

Next, we use the FO Taylor approximation of $(\boldsymbol{Y} + \Delta \boldsymbol{Y})^+$ for a tall matrix $\boldsymbol{Y} \in \mathbb{C}^{m \times n}$, i.e., $m > n$, given by

$$(\boldsymbol{Y} + \Delta \boldsymbol{Y})^+ \approx \boldsymbol{Y}^+ - \boldsymbol{Y}^+ \Delta \boldsymbol{Y} \boldsymbol{Y}^+ + \left(\boldsymbol{Y}^{\mathrm{H}} \boldsymbol{Y}\right)^{-1} \Delta \boldsymbol{Y}^{\mathrm{H}} \boldsymbol{P}_{\boldsymbol{Y}^\perp},$$

where $\boldsymbol{P}_{\boldsymbol{Y}^\perp} = \boldsymbol{I}_m - \boldsymbol{Y} \boldsymbol{Y}^+$. Using this property and inserting (4) into (7), we can express the SO truncated version of (7) as

$$\Delta \boldsymbol{\Psi} = \Delta \boldsymbol{\Psi}^{(1)} + \Delta \boldsymbol{\Psi}^{(2)} + \mathcal{O}\{\delta^3\}, \tag{8}$$

where

$$\Delta \boldsymbol{\Psi}^{(1)} = (\boldsymbol{J}_1 \boldsymbol{U}_{\mathrm{s}})^+ \left(\boldsymbol{J}_2 \Delta \boldsymbol{U}_{\mathrm{s}}^{(1)} - \boldsymbol{J}_1 \Delta \boldsymbol{U}_{\mathrm{s}}^{(1)} \boldsymbol{\Psi}\right), \tag{9}$$

$$\begin{aligned} \Delta \boldsymbol{\Psi}^{(2)} = &(\boldsymbol{J}_1 \boldsymbol{U}_{\mathrm{s}})^+ \left(\boldsymbol{J}_2 \Delta \boldsymbol{U}_{\mathrm{s}}^{(2)} - \boldsymbol{J}_1 \Delta \boldsymbol{U}_{\mathrm{s}}^{(2)} \boldsymbol{\Psi}\right) \\ &+ \Bigg(- (\boldsymbol{J}_1 \boldsymbol{U}_{\mathrm{s}})^+ \left(\boldsymbol{J}_1 \Delta \boldsymbol{U}_{\mathrm{s}}^{(1)}\right) (\boldsymbol{J}_1 \boldsymbol{U}_{\mathrm{s}})^+ \\ &+ \left((\boldsymbol{J}_1 \boldsymbol{U}_{\mathrm{s}})^{\mathrm{H}} (\boldsymbol{J}_1 \boldsymbol{U}_{\mathrm{s}})\right)^{-1} \left(\boldsymbol{J}_1 \Delta \boldsymbol{U}_{\mathrm{s}}^{(1)}\right)^{\mathrm{H}} \boldsymbol{P}_{(\boldsymbol{J}_1 \boldsymbol{U}_{\mathrm{s}})^\perp} \Bigg) \\ &\left(\boldsymbol{J}_2 \Delta \boldsymbol{U}_{\mathrm{s}}^{(1)} - \boldsymbol{J}_1 \Delta \boldsymbol{U}_{\mathrm{s}}^{(1)} \boldsymbol{\Psi}\right). \end{aligned} \tag{10}$$

3.3. Perturbation of the Eigenvalue Decomposition

Let the perturbed version of the noise-free eigendecomposition $\boldsymbol{\Psi} = \boldsymbol{Q} \boldsymbol{\Lambda} \boldsymbol{Q}^{-1}$ be given by

$$\hat{\boldsymbol{\Psi}} = \boldsymbol{\Psi} + \Delta \boldsymbol{\Psi} = (\boldsymbol{Q} + \Delta \boldsymbol{Q}) (\boldsymbol{\Lambda} + \Delta \boldsymbol{\Lambda}) (\boldsymbol{Q} + \Delta \boldsymbol{Q})^{-1}. \tag{11}$$

Approximating the term $(\boldsymbol{Q} + \Delta \boldsymbol{Q})^{-1}$ by its FO Taylor expansion $(\boldsymbol{Q} + \Delta \boldsymbol{Q})^{-1} \approx \boldsymbol{Q}^{-1} - \boldsymbol{Q}^{-1} \Delta \boldsymbol{Q} \boldsymbol{Q}^{-1}$, defining $\boldsymbol{P} = \boldsymbol{Q}^{-1}$, and solving (11) for $\Delta \boldsymbol{\Psi}$, its individual eigenvalue perturbation $\Delta \lambda_i,\ i = 1, \ldots, d$, up to the SO can be expressed as

$$\Delta \lambda_i = \boldsymbol{p}_i^{\mathrm{T}} \Delta \boldsymbol{\Psi} \boldsymbol{q}_i + \lambda_i (\boldsymbol{p}_i^{\mathrm{T}} \Delta \boldsymbol{q}_i)^2 + \mathcal{O}\{\delta^3\}, \tag{12}$$

where $\boldsymbol{p}_i^{\mathrm{T}}$ and $\boldsymbol{q}_i$ denote the i-th row of $\boldsymbol{P}$ and the i-th column of $\boldsymbol{Q}$, respectively. With the help of the eigenvector equation $\big((\boldsymbol{\Psi} + \Delta \boldsymbol{\Psi}) - (\lambda_i + \Delta \lambda_i) \boldsymbol{I}_d\big)(\boldsymbol{q}_i + \Delta \boldsymbol{q}_i) = \boldsymbol{0}$ solved for $\Delta \boldsymbol{q}_i$, it can be shown that the second term of (12) evaluates to zero. Therefore, the SO expansion of $\Delta \lambda_i$ is given by

$$\Delta \lambda_i = \Delta \lambda_i^{(1)} + \Delta \lambda_i^{(2)} + \mathcal{O}\{\delta^3\} \tag{13}$$

with $\Delta \lambda_i^{(1)} = \boldsymbol{p}_i^{\mathrm{T}} \Delta \boldsymbol{\Psi}^{(1)} \boldsymbol{q}_i$ and $\Delta \lambda_i^{(2)} = \boldsymbol{p}_i^{\mathrm{T}} \Delta \boldsymbol{\Psi}^{(2)} \boldsymbol{q}_i$.

3.4. Perturbation of the Spatial Frequency Estimates

The relation between the perturbed eigenvalues and the spatial frequency estimates is given by $\lambda_i + \Delta\lambda_i = \mathrm{e}^{\mathrm{j}(\mu_i + \Delta\mu_i)}$. Taking the logarithms of both sides and applying the SO Taylor approximation to the left hand side, we get

$$\ln(\lambda_i) + \frac{\Delta\lambda_i}{\lambda_i} - \frac{(\Delta\lambda_i)^2}{2\lambda_i^2} \approx \mathrm{j}(\mu_i + \Delta\mu_i). \tag{14}$$

Then, equating the imaginary parts of both sides, the SO expansion of $\Delta\mu_i$ is obtained as

$$\Delta\mu_i = \Delta\mu_i^{(1)} + \Delta\mu_i^{(2)} + \mathcal{O}\{\delta^3\} \tag{15}$$

with

$$\Delta\mu_i^{(1)} = \mathrm{Im}\left\{\Delta\lambda_i^{(1)}/\lambda_i\right\}, \tag{16}$$

$$\Delta\mu_i^{(2)} = \mathrm{Im}\left\{\Delta\lambda_i^{(2)}/\lambda_i\right\} - \frac{1}{2}\,\mathrm{Im}\left\{\left(\Delta\lambda_i^{(1)}\right)^2/\lambda_i^2\right\}. \tag{17}$$

Inserting the FO expressions from (5), (9), and (13) into (16), we immediately obtain the result for the FO spatial frequency error $\Delta\mu_i^{(1)}$ derived in [5], which is given by

$$\Delta\mu_i^{(1)} = \mathrm{Im}\left\{\boldsymbol{r}_i^{\mathrm{T}}\boldsymbol{W}\boldsymbol{n}\right\}, \tag{18}$$

where $\boldsymbol{n} = \mathrm{vec}\{\boldsymbol{N}\} \in \mathbb{C}^{MN\times 1}$ and

$$\boldsymbol{r}_i = \boldsymbol{q}_i \otimes \left(\left[(\boldsymbol{J}_1\boldsymbol{U}_\mathrm{s})^+ (\boldsymbol{J}_2/\lambda_i - \boldsymbol{J}_1)\right]^{\mathrm{T}} \boldsymbol{p}_i\right), \tag{19}$$

$$\boldsymbol{W} = \left(\boldsymbol{\Sigma}_\mathrm{s}^{-1}\boldsymbol{V}_\mathrm{s}^{\mathrm{T}}\right) \otimes \left(\boldsymbol{U}_\mathrm{n}\boldsymbol{U}_\mathrm{n}^{\mathrm{H}}\right). \tag{20}$$

Upon inserting the expressions for (4), (8), and (13) into (17), the SO term of the spatial frequency error $\Delta\mu_i^{(2)}$ can be compactly expressed as

$$\Delta\mu_i^{(2)} = \mathrm{Im}\left\{\boldsymbol{n}^{\mathrm{H}}\boldsymbol{A}_i\boldsymbol{n} + \boldsymbol{n}^{\mathrm{T}}\boldsymbol{B}_i\boldsymbol{n}\right\}, \tag{21}$$

where the matrices $\boldsymbol{A}_i$ and $\boldsymbol{B}_i$ are defined as

$$\begin{aligned}\boldsymbol{A}_i = &\left(\boldsymbol{V}_\mathrm{n}\boldsymbol{V}_\mathrm{n}^{\mathrm{H}}\right)^{\mathrm{T}} \otimes \left(\boldsymbol{U}_\mathrm{s}\boldsymbol{\Sigma}_\mathrm{s}^{-2}\boldsymbol{q}_i\boldsymbol{p}_i^{\mathrm{T}}(\boldsymbol{J}_1\boldsymbol{U}_\mathrm{s})^+(\boldsymbol{J}_2/\lambda_i - \boldsymbol{J}_1)\,\boldsymbol{U}_\mathrm{n}\boldsymbol{U}_\mathrm{n}^{\mathrm{H}}\right)\\ &+ \left(\boldsymbol{p}_i^{\mathrm{T}}\left((\boldsymbol{J}_1\boldsymbol{U}_\mathrm{s})^{\mathrm{H}}(\boldsymbol{J}_1\boldsymbol{U}_\mathrm{s})\right)^{-1}\boldsymbol{\Sigma}_\mathrm{s}^{-1}\boldsymbol{V}_\mathrm{s}^{\mathrm{H}}\right)^{\mathrm{T}}\left(\boldsymbol{V}_\mathrm{s}\boldsymbol{\Sigma}_\mathrm{s}^{-1}\boldsymbol{q}_i\right)^{\mathrm{T}}\\ &\otimes \left(\boldsymbol{U}_\mathrm{n}\boldsymbol{U}_\mathrm{n}^{\mathrm{H}}\boldsymbol{J}_1^{\mathrm{T}}\boldsymbol{P}_{(\boldsymbol{J}_1\boldsymbol{U}_\mathrm{s})^\perp}(\boldsymbol{J}_2/\lambda_i - \boldsymbol{J}_1)\,\boldsymbol{U}_\mathrm{n}\boldsymbol{U}_\mathrm{n}^{\mathrm{H}}\right),\end{aligned} \tag{22}$$

$$\begin{aligned}\boldsymbol{B}_i = &-\boldsymbol{K}_{M,N}^{\mathrm{T}}\left(\left(\boldsymbol{X}_0^+\right)^{\mathrm{T}} \otimes \left(\boldsymbol{V}_\mathrm{s}\boldsymbol{\Sigma}_\mathrm{s}^{-1}\boldsymbol{q}_i\right)\right.\\ &\left.\otimes \left(\boldsymbol{p}_i^{\mathrm{T}}(\boldsymbol{J}_1\boldsymbol{U}_\mathrm{s})^+(\boldsymbol{J}_2/\lambda_i - \boldsymbol{J}_1)\,\boldsymbol{U}_\mathrm{n}\boldsymbol{U}_\mathrm{n}^{\mathrm{H}}\right)\right)\\ &-\boldsymbol{K}_{M,N}^{\mathrm{T}}\left(\left(\boldsymbol{V}_\mathrm{s}\boldsymbol{\Sigma}_\mathrm{s}^{-1}(\boldsymbol{J}_1\boldsymbol{U}_\mathrm{s})^+(\boldsymbol{J}_2/\lambda_i - \boldsymbol{J}_1)\,\boldsymbol{U}_\mathrm{n}\boldsymbol{U}_\mathrm{n}^{\mathrm{H}}\right)^{\mathrm{T}}\right.\\ &\left.\otimes \left(\boldsymbol{V}_\mathrm{s}\boldsymbol{\Sigma}_\mathrm{s}^{-1}\boldsymbol{q}_i\boldsymbol{p}_i^{\mathrm{T}}(\boldsymbol{J}_1\boldsymbol{U}_\mathrm{s})^+\boldsymbol{J}_1\boldsymbol{U}_\mathrm{n}\boldsymbol{U}_\mathrm{n}^{\mathrm{H}}\right)\right) - \frac{1}{2}\left(\boldsymbol{r}_i^{\mathrm{T}}\boldsymbol{W}\right)^{\mathrm{T}}\left(\boldsymbol{r}_i^{\mathrm{T}}\boldsymbol{W}\right)\end{aligned} \tag{23}$$

with $\boldsymbol{K}_{M,N} \in \mathbb{R}^{MN\times MN}$ being the commutation matrix that satisfies $\boldsymbol{K}_{M,N}\cdot\mathrm{vec}\{\boldsymbol{A}\} = \mathrm{vec}\{\boldsymbol{A}^{\mathrm{T}}\}$ for arbitrary matrices $\boldsymbol{A} \in \mathbb{C}^{M\times N}$ [12]. Note that for the derivation of (21), we have used the following properties for matrices of appropriate sizes:

$$\mathrm{Tr}\left\{\boldsymbol{A}\boldsymbol{X}\boldsymbol{B}\boldsymbol{X}^{\mathrm{H}}\boldsymbol{C}^{\mathrm{H}}\right\} = \mathrm{vec}\{\boldsymbol{X}\}^{\mathrm{H}}\left(\boldsymbol{B}^{\mathrm{T}} \otimes \left(\boldsymbol{C}^{\mathrm{H}}\boldsymbol{A}\right)\right)\mathrm{vec}\{\boldsymbol{X}\},$$

$$\mathrm{Tr}\{\boldsymbol{A}\boldsymbol{X}\boldsymbol{B}\boldsymbol{X}\boldsymbol{C}\} = \mathrm{vec}\{\boldsymbol{X}\}^{\mathrm{T}}\boldsymbol{K}_{M,N}^{\mathrm{T}}\left(\boldsymbol{B}^{\mathrm{T}} \otimes (\boldsymbol{C}\boldsymbol{A})\right)\mathrm{vec}\{\boldsymbol{X}\},$$

$$\mathrm{Tr}\left\{\boldsymbol{A}^{\mathrm{H}}\boldsymbol{X}^{\mathrm{H}}\boldsymbol{B}\boldsymbol{X}\boldsymbol{C}\right\} = \mathrm{vec}\{\boldsymbol{X}\}^{\mathrm{H}}\left(\left(\boldsymbol{A}^*\boldsymbol{C}^{\mathrm{T}}\right) \otimes \boldsymbol{B}\right)\mathrm{vec}\{\boldsymbol{X}\}.$$

These identities can be easily proven by applying the common trace and the vectorization properties along with the commutation matrix rule.

3.5. MSE Expression of Standard ESPRIT

For the derivation of the analytical MSE expression for Standard ESPRIT, we assume for simplicity that the noise is zero-mean circularly symmetric complex Gaussian, i.e., the covariance matrix $\boldsymbol{R}_{\mathrm{nn}} = \mathbb{E}\{\boldsymbol{n}\boldsymbol{n}^{\mathrm{H}}\}$ and the pseudo-covariance matrix $\boldsymbol{C}_{\mathrm{nn}} = \mathbb{E}\{\boldsymbol{n}\boldsymbol{n}^{\mathrm{T}}\}$ of $\boldsymbol{n} \in \mathbb{C}^{MN\times 1}$ simplify to $\boldsymbol{R}_{\mathrm{nn}} = \sigma_\mathrm{n}^2\boldsymbol{I}_{MN}$ and $\boldsymbol{C}_{\mathrm{nn}} = \boldsymbol{0}_{MN}$.

Then, the MSE for the i-th spatial frequency is given by

$$\begin{aligned}\mathbb{E}\left\{(\Delta\mu_i)^2\right\} \approx\ &\mathbb{E}\left\{\left(\Delta\mu_i^{(1)}\right)^2\right\} + 2\cdot\mathbb{E}\left\{\Delta\mu_i^{(1)}\Delta\mu_i^{(2)}\right\}\\ &+ \mathbb{E}\left\{\left(\Delta\mu_i^{(2)}\right)^2\right\} + \mathcal{O}\{\delta^6\},\end{aligned} \tag{24}$$

where the first term of (24) is already known from the analytical FO MSE expression in [5] and given as

$$\mathbb{E}\left\{\left(\Delta\mu_i^{(1)}\right)^2\right\} = \frac{\sigma_\mathrm{n}^2}{2}\left\|\boldsymbol{W}^{\mathrm{T}}\boldsymbol{r}_i\right\|_2^2. \tag{25}$$

The second term of (24) can be written as

$$\begin{aligned}2\cdot\mathbb{E}\left\{\Delta\mu_i^{(1)}\Delta\mu_i^{(2)}\right\} = &\ 2\cdot\mathbb{E}\left\{\mathrm{Im}\left\{\boldsymbol{r}_i^{\mathrm{T}}\boldsymbol{W}\boldsymbol{n}\right\}\mathrm{Im}\left\{\boldsymbol{n}^{\mathrm{H}}\boldsymbol{A}_i\boldsymbol{n}\right\}\right\}\\ &+ 2\cdot\mathbb{E}\left\{\mathrm{Im}\left\{\boldsymbol{r}_i^{\mathrm{T}}\boldsymbol{W}\boldsymbol{n}\right\}\mathrm{Im}\left\{\boldsymbol{n}^{\mathrm{T}}\boldsymbol{B}_i\boldsymbol{n}\right\}\right\}\end{aligned} \tag{26}$$

and evaluates to zero. This results from the zero-mean and the circularity of the noise. The third term of (24) can be expressed as

$$\begin{aligned}\mathbb{E}\left\{\left(\Delta\mu_i^{(2)}\right)^2\right\} &= \mathbb{E}\left\{\left(\mathrm{Im}\left\{\boldsymbol{n}^{\mathrm{H}}\boldsymbol{A}_i\boldsymbol{n}\right\} + \mathrm{Im}\left\{\boldsymbol{n}^{\mathrm{T}}\boldsymbol{B}_i\boldsymbol{n}\right\}\right)^2\right\}\\ &= \mathbb{E}\left\{\mathrm{Im}\left\{\boldsymbol{n}^{\mathrm{H}}\boldsymbol{A}_i\boldsymbol{n}\right\}^2\right\} + 2\cdot\mathbb{E}\left\{\mathrm{Im}\left\{\boldsymbol{n}^{\mathrm{H}}\boldsymbol{A}_i\boldsymbol{n}\right\}\mathrm{Im}\left\{\boldsymbol{n}^{\mathrm{T}}\boldsymbol{B}_i\boldsymbol{n}\right\}\right\}\\ &\quad + \mathbb{E}\left\{\mathrm{Im}\left\{\boldsymbol{n}^{\mathrm{T}}\boldsymbol{B}_i\boldsymbol{n}\right\}^2\right\}.\end{aligned} \tag{27}$$

Note that the middle term of (27) is again equal to zero due to the assumptions on the noise. The first term can be simplified to

$$\begin{aligned}\mathbb{E}\left\{\mathrm{Im}\left\{\boldsymbol{n}^{\mathrm{H}}\boldsymbol{A}_i\boldsymbol{n}\right\}^2\right\} &= \frac{1}{4}\,\mathbb{E}\left\{\left(-\mathrm{j}\boldsymbol{n}^{\mathrm{H}}\boldsymbol{A}_i\boldsymbol{n} + \mathrm{j}\boldsymbol{n}^{\mathrm{T}}\boldsymbol{A}_i^*\boldsymbol{n}^*\right)^2\right\}\\ &= \frac{1}{2}\big(\mathrm{Re}\{E_2\} - \mathrm{Re}\{E_1\}\big)\end{aligned} \tag{28}$$

with $E_1 = \mathbb{E}\left\{\boldsymbol{n}^{\mathrm{H}}\boldsymbol{A}_i\boldsymbol{n}\boldsymbol{n}^{\mathrm{H}}\boldsymbol{A}_i\boldsymbol{n}\right\}$ and $E_2 = \mathbb{E}\left\{\boldsymbol{n}^{\mathrm{H}}\boldsymbol{A}_i\boldsymbol{n}\boldsymbol{n}^{\mathrm{T}}\boldsymbol{A}_i^*\boldsymbol{n}^*\right\}$. Then, it can be shown after straightforward calculations based on [13] that

$$E_1 = \sigma_\mathrm{n}^4\left(\mathrm{Tr}\{\boldsymbol{A}_i\}^2 + \mathrm{Tr}\left\{\boldsymbol{A}_i^2\right\}\right), \tag{29}$$

$$E_2 = \sigma_\mathrm{n}^4\left(|\,\mathrm{Tr}\{\boldsymbol{A}_i\}|^2 + \mathrm{Tr}\left\{\boldsymbol{A}_i^{\mathrm{H}}\boldsymbol{A}_i\right\}\right). \tag{30}$$

Analogously, the third term of (27) is given by

$$\begin{aligned}\mathbb{E}\left\{\mathrm{Im}\left\{\boldsymbol{n}^{\mathrm{T}}\boldsymbol{B}_i\boldsymbol{n}\right\}^2\right\} &= \frac{1}{4}\,\mathbb{E}\left\{\left(-\mathrm{j}\boldsymbol{n}^{\mathrm{T}}\boldsymbol{B}_i\boldsymbol{n} + \mathrm{j}\boldsymbol{n}^{\mathrm{H}}\boldsymbol{B}_i^*\boldsymbol{n}^*\right)^2\right\}\\ &= \frac{1}{2}\big(\mathrm{Re}\{F_2\} - \mathrm{Re}\{F_1\}\big)\end{aligned} \tag{31}$$

with $F_1 = \mathbb{E}\left\{\boldsymbol{n}^{\mathrm{T}}\boldsymbol{B}_i\boldsymbol{n}\boldsymbol{n}^{\mathrm{T}}\boldsymbol{B}_i\boldsymbol{n}\right\}$ and $F_2 = \mathbb{E}\left\{\boldsymbol{n}^{\mathrm{T}}\boldsymbol{B}_i\boldsymbol{n}\boldsymbol{n}^{\mathrm{H}}\boldsymbol{B}_i^{*}\boldsymbol{n}^{*}\right\}$. Again, F_1 evaluates to zero due to the circularity of the noise, while F_2 can be shown to be equal to

$$F_2 = \sigma_{\mathrm{n}}^4 \,\mathrm{Tr}\left\{\boldsymbol{B}_i^{\mathrm{H}}\left(\boldsymbol{B}_i + \boldsymbol{B}_i^{\mathrm{T}}\right)\right\}. \tag{32}$$

Consequently, the MSE of the SO terms in (27) becomes

$$\mathbb{E}\left\{\left(\Delta\mu_i^{(2)}\right)^2\right\} = \frac{\sigma_{\mathrm{n}}^4}{2}\left(|\,\mathrm{Tr}\left\{\boldsymbol{A}_i\right\}|^2 + \mathrm{Tr}\left\{\boldsymbol{A}_i^{\mathrm{H}}\boldsymbol{A}_i\right\}\right.$$
$$\left. - \,\mathrm{Re}\left\{\mathrm{Tr}\left\{\boldsymbol{A}_i\right\}^2 + \mathrm{Tr}\left\{\boldsymbol{A}_i^2\right\}\right\} + \mathrm{Tr}\left\{\boldsymbol{B}_i^{\mathrm{H}}\left(\boldsymbol{B}_i + \boldsymbol{B}_i^{\mathrm{T}}\right)\right\}\right). \tag{33}$$

Eventually, we insert (25) and (33) into (24) and obtain the final expression for (24) of the i-th spatial frequency as

$$\mathbb{E}\left\{(\Delta\mu_i)^2\right\} \approx \frac{\sigma_{\mathrm{n}}^2}{2}\left\|\boldsymbol{W}^{\mathrm{T}}\boldsymbol{r}_i\right\|_2^2 + \frac{\sigma_{\mathrm{n}}^4}{2}\left(|\mathrm{Tr}\left\{\boldsymbol{A}_i\right\}|^2 + \mathrm{Tr}\left\{\boldsymbol{A}_i^{\mathrm{H}}\boldsymbol{A}_i\right\}\right.$$
$$\left. + \,\mathrm{Tr}\left\{\boldsymbol{B}_i^{\mathrm{H}}\left(\boldsymbol{B}_i + \boldsymbol{B}_i^{\mathrm{T}}\right)\right\} - \mathrm{Re}\left\{\mathrm{Tr}\left\{\boldsymbol{A}_i\right\}^2 + \mathrm{Tr}\left\{\boldsymbol{A}_i^2\right\}\right\}\right), \tag{34}$$

where $\boldsymbol{r}_i$ and $\boldsymbol{W}$ are given in (19) and (20), and $\boldsymbol{A}_i$ and $\boldsymbol{B}_i$ are defined in (22) and (23), respectively.

3.6. Threshold SNR for the Threshold Region

Besides performance prediction and comparison purposes, the derived FO and SO analytical MSE expressions can also be used to compute the SNR threshold that characterizes the MSE threshold region. To this end, we set both MSE expressions equal to each other and compute the 3-dB cutoff SNR threshold, which corresponds to the SNR where the MSE exceeds its FO prediction by 3 dB. Specifically, we first compute the cutoff noise power as

$$\sigma_{3\mathrm{dB}}^2 = \mathbb{E}\left\{\left(\Delta\mu_i^{(1)}\right)^2\right\} = \mathbb{E}\left\{\left(\Delta\mu_i^{(2)}\right)^2\right\} \tag{35}$$
$$= \left\|\boldsymbol{W}^{\mathrm{T}}\boldsymbol{r}_i\right\|_2^2 \Big/ \left(|\mathrm{Tr}\left\{\boldsymbol{A}_i\right\}|^2 + \mathrm{Tr}\left\{\boldsymbol{A}_i^{\mathrm{H}}\boldsymbol{A}_i\right\}\right.$$
$$\left. + \,\mathrm{Tr}\left\{\boldsymbol{B}_i^{\mathrm{H}}\left(\boldsymbol{B}_i + \boldsymbol{B}_i^{\mathrm{T}}\right)\right\} - \mathrm{Re}\left\{\mathrm{Tr}\left\{\boldsymbol{A}_i\right\}^2 + \mathrm{Tr}\left\{\boldsymbol{A}_i^2\right\}\right\}\right),$$

which is then used to compute the SNR threshold according to $\mathrm{SNR}_{3\mathrm{dB}} = 10\lg\left(P_{\mathrm{s}}/\sigma_{3\mathrm{dB}}^2\right)$, where P_{s} is the signal power.

4. SIMULATION RESULTS

In this section, we provide numerical results to evaluate the behavior of the presented analytical SO performance framework of 1-D Standard ESPRIT (SE). In particular, we compare the derived analytical MSE expression in (34) "SE ana (1+2)" to the empirical "SE emp" estimation errors of the algorithm obtained by averaging over Monte Carlo trials. Additionally, we also include the analytical FO MSE expression in (25) "SE ana (1)" known from [5] and the SO only MSE expression "SE ana (2)" in (33). The overall performance is benchmarked by the deterministic CRB (Det CRB) [14]. For the simulations, we adopt a uniform linear array (ULA) composed of $M = 10$ isotropic sensors with half-wavelength spacing. The d impinging signals carry QPSK-modulated symbols with unit power. Moreover, we assume the noise to be circularly symmetric white Gaussian. The curves are obtained by averaging over 5000 trials.

Fig. 1 shows the total RMSE over all sources as a function of the SNR. We assume $d = 2$ signals at the positions $\mu_1 = 0.7$ and $\mu_2 = 0.8$ with a real-valued pair-wise correlation of $\rho = 0.8$. The number of snapshots is $N = 20$. It is apparent from Fig. 1 that the analytical curve "SE ana (1+2)" coincides with "SE ana (1)" and

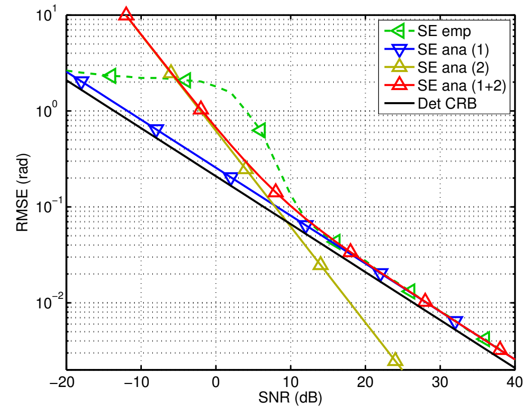

Fig. 1. RMSE versus SNR for $M = 10$, $N = 20$, $d = 2$ correlated sources ($\rho = 0.8$) at $\mu_1 = 0.7$ and $\mu_2 = 0.8$.

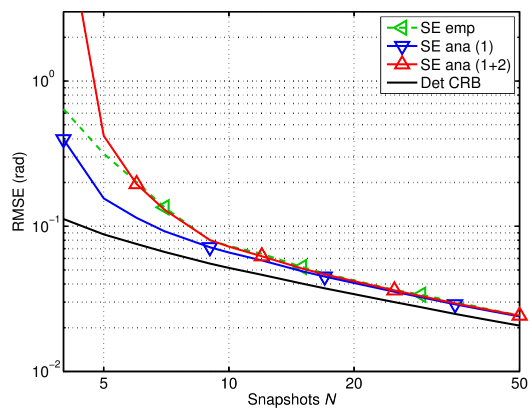

Fig. 2. RMSE versus snapshots N for $M = 10$, SNR = 20 dB, $d = 3$ uncorrelated sources at $\mu_1 = 0$, $\mu_2 = 0.25$, and $\mu_3 = 0.5$.

both agree well with "SE emp" in the high SNR regime. At lower SNRs, "SE ana (1+2)" accurately models the behavior of "SE emp" at the start of the threshold region. The 3-dB SNR threshold, i.e., the intersection of "SE ana (1)" and "SE ana (2)" can be computed analytically using (35).

In Fig. 2, we illustrate the RMSE versus the number of snapshots N. We assume $d = 3$ uncorrelated signals at $\mu_1 = 0$, $\mu_2 = 0.25$, and $\mu_3 = 0.5$. The SNR is fixed at 20 dB. Again, we observe hat the analytical curves and the empirical curves match well for a large sample size N and "SE ana (1+2)" accurately models the algorithmic behavior of "SE emp" for a small sample size.

5. CONCLUSION

In this paper, we have presented an SO analytical performance analysis of 1-D Standard ESPRIT. We have derived a closed-form expression for the parameter estimation error up to the SO and found an analytical MSE expression under the assumption of a zero-mean circularly symmetric complex Gaussian noise distribution. The advantage of these new SO expressions over the existing FO expressions is that they are not only valid in the high effective SNR region but also in a wider effective SNR range. Moreover, we have used the existing FO MSE expression and the derived SO MSE expression to analytically compute the SNR threshold of the MSE threshold region. The analytical expressions have been verified by empirical simulations.

6. REFERENCES

[1] R. H. Roy and T. Kailath, "ESPRIT-estimation of signal parameters via rotational invariance techniques," *IEEE Transactions on Acoustics, Speech, and Signal Processing*, vol. 37, no. 7, pp. 984-995, July 1989.

[2] M. Haardt and J. A. Nossek, "Unitary ESPRIT: How to obtain increased estimation accuracy with a reduced computational burden," *IEEE Transactions on Signal Processing*, vol. 43, no. 5, pp. 1232-1242, May 1995.

[3] B. D. Rao and K. V. S. Hari, "Performance analysis of ESPRIT and TAM in determining the direction of arrival of plane waves in noise," *IEEE Transactions on Acoustics, Speech, and Signal Processing*, vol. 37, no. 12, pp. 1990-1995, Dec. 1989.

[4] F. Li, H. Liu, and R. J. Vaccaro, "Performance analysis for DOA estimation algorithms: Unification, simplifications, and observations," *IEEE Transactions on Aerospace and Electronic Systems*, vol. 29, no. 4, pp. 1170-1184, Oct. 1993.

[5] F. Roemer, M. Haardt, and G. Del Galdo, "Analytical performance assessment of multi-dimensional matrix- and tensor-based ESPRIT-type algorithms," *IEEE Transactions on Signal Processing*, vol. 62, pp. 2611–2625, May 2014.

[6] J. Steinwandt, F. Roemer, M. Haardt, and G. Del Galdo, "R-dimensional ESPRIT-type algorithms for strictly second-order non-circular sources and their performance analysis," *IEEE Transactions on Signal Processing*, vol. 62, no. 18, pp. 4824-4838, Sep. 15, 2014.

[7] F. Li and Y. Lu, "Bias analysis for ESPRIT-type estimation algorithms," *IEEE Transactions on Antennas and Propagation*, vol. 42, no. 3, pp. 418-423, Mar 1994.

[8] Z. Xu, "Perturbation analysis for subspace decomposition with applications in subspace-based algorithms," *IEEE Transactions on Signal Processing*, vol. 50, no. 11, pp. 2820-2830, Nov. 2012.

[9] A. Ferreol, P. Larzabal, and M. Viberg, "On the asymptotic performance analysis of subspace DOA estimation in the presence of modeling errors: Case of MUSIC," *IEEE Transactions on Signal Processing*, vol. 54, no. 3, pp. 907-920, Mar. 2006.

[10] P. Forster, P. Larzabal, and E. Boyer, "Threshold performance analysis of maximum likelihood DOA estimation," *IEEE Transactions on Signal Processing*, vol. 52, no. 11, pp. 3183-3191, Nov. 2004.

[11] E. Chaumette, J. Galy, A. Quinlan, P. Larzabal, "A new Barankin bound approximation for the prediction of the threshold region performance of Maximum-Likelihood estimators," *IEEE Transactions on Signal Processing*, vol. 56, no. 11, pp. 5319-5333, Nov. 2008.

[12] J. R. Magnus and H. Neudecker, *Matrix differential calculus with applications in statistics and econometrics*, John Wiley and Sons, 1995.

[13] J. R. Magnus and H. Neudecker, "The commutation matrix: Some properties and applications," *Annals of Statistics*, vol. 7, no. 2, pp. 381-394, Mar. 1979.

[14] P. Stoica and A. Nehorai, "MUSIC, maximum likelihood, and Cramer-Rao bound," *IEEE Transactions on Acoustics, Speech, and Signal Processing*, vol. 37, no. 5, pp. 720-741, May 1989.